Innovative: International Multi-disciplinary Journal of Applied Technology
(ISSN 2995-486X) VOLUME 03 ISSUE 11, 2025

REMOVAL OF MO, SE, U, AS AND V OXYANIONS FROM SALINE GROUNDWATER AND AGRICULTURAL DRAINAGE WATER BY ACTIVATED TEBINBULAK TITANOMAGNETITE: DOSE–RESPONSE BEHAVIOUR, SELECTIVITY SEQUENCE AND THE ROLE OF THE ALKALINE PRE-TREATMENT REAGENT

Ergashev Muhsinjon Ergashevich
Department of Agronomy, Navoi State University of Mining and Technologies, Navoi, Uzbekistan

Shodiqulov Jurabek Mehriqulovich (Corresponding Author)
Department of Agronomy, Navoi State University of Mining and Technologies, Navoi, Uzbekistan
Email: shodiqulov_jurabek@mail.ru

Doniyorov Kamoliddin Alouddinovich
Department of Agronomy, Navoi State University of Mining and Technologies, Navoi, Uzbekistan

Abstract:
Drainage and shallow groundwater of the Kyzylkum region (Uzbekistan) carry molybdenum, uranium and selenium at 1.1–14 times the FAO/WHO irrigation guidelines in a sulphate–chloride matrix of 8.2–8.5 g L^{-1} dry residue. This study quantifies the batch removal of Mo, Se, U, As and V oxyanions from two such waters by a sorbent made from Tebinbulak titanomagnetite ore, after alkaline pre-treatment with KOH, NH_3 or $Ca(OH)_2$ to pH 7.5–8.0, over seven sorbent doses (0.5–10 g L^{-1}). Rather than reporting removal percentages alone, the 42 dose–response curves were reduced to a first-order saturation model $\eta = \eta max(1 - e{-}kD)$ ($R^2 \geq 0.999$), whose rate constant k (L g^{-1}) and derived characteristic doses $D_{50} = \ln 2/k$ and $D_{90} = \ln 10/k$ provide a compact, reagent- and element-specific description. k ranked the oxyanions in the invariant order As > V > Mo > U > Se (0.94, 0.81, 0.70, 0.62, 0.54 L g^{-1} after KOH) and the pre-treatment reagents in the order $Ca(OH)_2$ > KOH > NH_3 (for Mo: 0.88, 0.70, 0.55 L g^{-1}), so that D_{90} ranged from 1.9 g L^{-1} (As, lime) to 5.2 g L^{-1} (Se, ammonia). The two waters gave the same removal fractions within the 1 % resolution of the data, their difference lying in residual concentrations: molybdenum (initial 140 µg L^{-1}) limits the groundwater and requires 4 g L^{-1} after lime, 6 g L^{-1} after KOH and 10 g L^{-1} after ammonia to meet the FAO limit of 10 µg L^{-1}, whereas uranium limits the drainage water and is met at 2 g L^{-1}. Specific uptake fell from 55–80 to 11 µg Mo g^{-1} across the dose range, marking 6 g L^{-1} as the point beyond which sorbent is wasted. A dose window of 4–6 g L^{-1} with lime pre-treatment is recommended for returning both waters to irrigation.

Keywords: oxyanions; molybdenum; uranium; selenium; arsenic; vanadium; titanomagnetite; dose–response model; alkaline pre-treatment; drainage water reuse

Introduction

In the lower Amu Darya basin the only water resource that is growing is return flow from irrigation, and its reuse has become a necessity rather than an option [1][2][3][4]. Return flows of the Kyzylkum region, however, carry trace elements leached from soils and parent rock: molybdenum at 23–140 μg L^{-1} against an FAO irrigation limit of 10 μg L^{-1}, uranium at 74–75 μg L^{-1} against the WHO value of 30 μg L^{-1}, selenium at 22–33 μg L^{-1} against 20 μg L^{-1}, and arsenic close to the 10 μg L^{-1} guideline [5],[6]. The Kesterson episode in California remains the reference case for what drainage-borne selenium can do to a food chain [7],[8]; analogous risks have been documented for Central Asian irrigation systems [9],[10].

The chemistry of these elements at pH 7–8 is anionic — molybdate, selenite/selenate, uranyl–carbonate, arsenate and vanadate species [11][12][13]14] — and this is what makes them persistent. Lime or caustic treatment removes trivalent cations almost quantitatively at pH 7–8 but has no hold on anions [15], and in calcareous waters uranium is further protected by Ca–UO_2–CO_3 ternary complexes [16][17]. A separate anion-selective step is therefore unavoidable, and iron (hydr)oxides are its natural candidates: arsenate, selenite, molybdate and vanadate bind to ≡Fe–OH sites as inner-sphere complexes [18], while magnetite adds reductive immobilisation of U(VI), Se(IV/VI) and V(V) by lattice Fe^{2+} [19] and magnetic recoverability [20].

What the literature does not supply are dose–response data for an ore-derived magnetite sorbent in real brackish water, where sulphate at ≈3.6 g L^{-1}, chloride and bicarbonate compete for sites and loadings are in the microgram range. Our previous work produced such a sorbent from Tebinbulak titanomagnetite (3.5–4.3 Gt of ore in Karakalpakstan) with a BET area of 23.67 m^2 g^{-1} after thermal activation at 700 °C/2 h and up to 94 m^2 g^{-1} after mechanical activation. The present paper reports its performance in the sorption stage of a two-stage treatment. The approach taken is to describe each dose–response curve with a two-parameter saturation model, so that selectivity, the influence of the pre-treatment reagent and the dose needed for guideline compliance can all be read from a single rate constant rather than from tables of percentages.

Materials and Methods

Two waters typical of the region were used: an agricultural drainage water (collector Zakhkash) and a shallow groundwater (well Kuduk). Both are of sulphate–chloride–sodium type; their major-ion composition and trace-element content are summarised in Table 1. Major ions were determined by titrimetry and gravimetry, trace elements by ICP-MS.

Table 1. Composition of the raw waters and guideline values.

Parameter	Groundwater	Drainage water	Guideline (source)
pH	6.40	6.70	—
Dry residue, mg L^{-1}	8200	8500	—
SO_4^{2-} / Cl^- / HCO_3^-, mg L^{-1}	3683 / 1507 / 153	3638 / 1684 / 458	—
Ca^{2+} / Mg^{2+}, mg L^{-1}	551 / 274	551 / 298	—
Mo, μg L^{-1}	140	23	10 (FAO [5])
Se, μg L^{-1}	33	22	20 (FAO [5])
U, μg L^{-1}	74	75	30 (WHO [6])
As, μg L^{-1}	9.8	8.1	10 (WHO [6])
V, μg L^{-1}	5.2	4.5	—

The sorbent was prepared from Tebinbulak titanomagnetite ore (15–17 % Fe; 63.5 % Fe in the magnetic concentrate) by crushing, ball-milling and activation as described elsewhere; the thermally activated material (700 °C, 2.0 h) has a BET area of 23.67 $m^2\ g^{-1}$, an external surface of 18.80 $m^2\ g^{-1}$, a pore volume of 0.120 $cm^3\ g^{-1}$ and a crystallite size of 64.86 nm. Its point of zero charge is ≈6.5, so that at pH 7.5–8.0 the surface is slightly negative and anion uptake relies on ligand exchange rather than electrostatics [18],[19].

One-litre samples were brought to pH 7.5–8.0 under stirring with 1 M KOH, 5 % NH_3 or 5 % $Ca(OH)_2$ slurry, mixed rapidly (2–3 min) and slowly (15–20 min), settled and membrane-filtered. The filtrates, whose oxyanion content C_0 is listed in Table 2, were the feeds of the sorption stage. Pre-treatment left 83–89 % of the raw-water Mo, Se, U, As and V in solution, slightly more after NH_3 than after the two strong bases.

Table 2. Oxyanion content of the sorption-stage feeds (after pre-treatment), μg L^{-1}.

Reagent	Water	Mo	Se	U	As	V
KOH	Groundwater	116.40	25.08	57.24	7.05	3.75
KOH	Drainage	17.08	16.12	57.00	6.06	3.48
NH_3	Groundwater	125.40	29.38	64.64	8.43	4.47
NH_3	Drainage	21.78	19.92	63.50	6.97	3.87
$Ca(OH)_2$	Groundwater	118.00	27.40	59.20	7.94	4.16
$Ca(OH)_2$	Drainage	17.40	16.60	61.25	6.28	3.60

Batch contacts were run at doses D = 0.5, 1.0, 2.0, 4.0, 6.0, 8.0 and 10.0 g L^{-1} for each of the six feeds (42 runs); after magnetic separation and filtration the five elements were determined by ICP-MS. Removal $\eta = (C_0 - C)/C_0 \cdot 100$ % was recorded to the nearest 1 %. Each dose–response curve was fitted by non-linear least squares to the first-order saturation model

$$\eta(D) = \eta_{max}(1 - e^{-kD})$$

in which η_{max} is the asymptotic removal and k (L g^{-1}) measures how quickly it is approached. Two characteristic doses follow from k:

$$D_{50} = \frac{\ln 2}{k}; \qquad D_{90} = \frac{\ln 10}{k}$$

i.e. the doses at which 50 % and 90 % of η_{max} are reached. Residual concentrations were obtained as $C = C_0(1 - \eta/100)$ and specific uptake as

$$q = \frac{C_0\,\eta}{100\,D}$$

(μg of element per g of sorbent). The model was preferred to a hyperbolic (Langmuir-type) form, which fitted less well (R^2 = 0.96–0.99) and overestimated η_{max}.

Results

All 30 curves obtained for the groundwater (five elements × three reagents; Table 3 gives the KOH series, Fig. 1 plots it) and the corresponding drainage-water curves are described by the saturation model with $R^2 \geq 0.999$; the fitted parameters are collected in Table 4. The quality of the fit means that the entire data set can be discussed in terms of two numbers per element and reagent. η_{max} lies between 89 and 99 % and sets the ceiling that no amount of sorbent will exceed in a single contact; k sets how much sorbent is needed to approach it.

Table 3. Removal η (%) from KOH-pre-treated groundwater versus sorbent dose.

Dose, g L^{-1}	0.5	1.0	2.0	4.0	6.0	8.0	10.0
Mo	28	48	72	89	94	95	95
Se	22	39	61	82	89	91	92
U	25	43	67	86	92	93	94

Dose, g L^{-1}	0.5	1.0	2.0	4.0	6.0	8.0	10.0
As	37	60	83	96	98	98	98
V	32	53	77	92	95	96	96

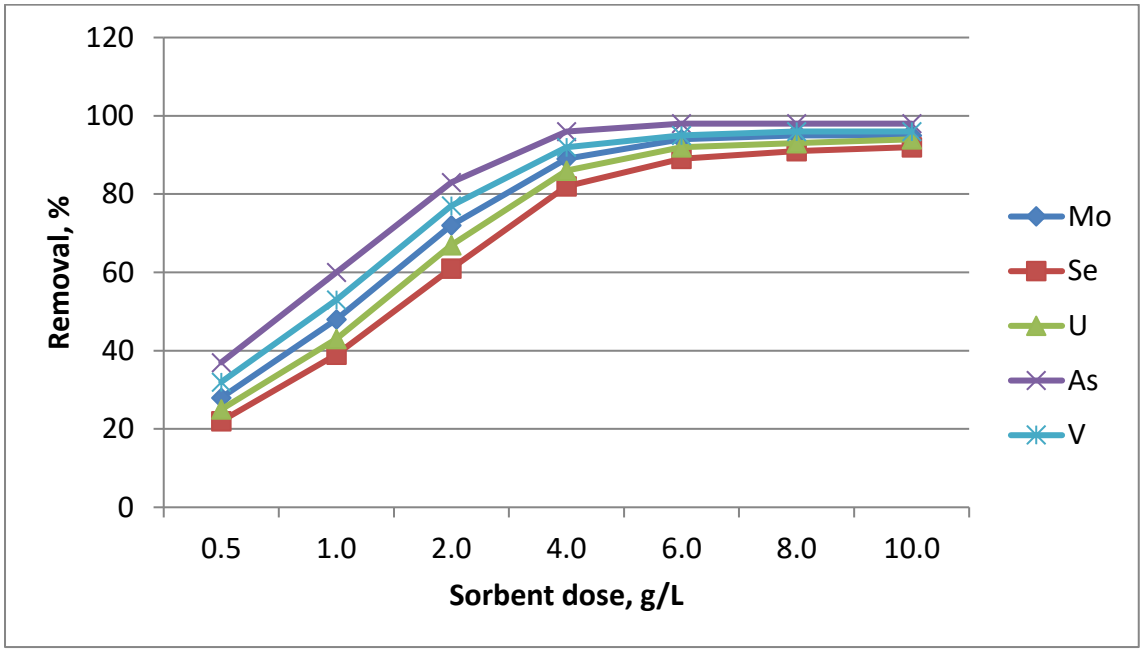


Figure 1. Dose–response curves for Mo, Se, U, As and V in KOH-pre-treated groundwater (points: experiment; the saturation model passes through them within ±1 %).

Table 4. Parameters of the saturation model $\eta = \eta_{max}(1 - e^{-kD})$ and characteristic doses for groundwater (identical removal fractions were obtained for the drainage water).

Reagent	Element	η_{max}, %	k, L g^{-1}	D_{50}, g L^{-1}	D_{90}, g L^{-1}
KOH	As	98.1	0.943	0.74	2.44
KOH	V	96.0	0.807	0.86	2.85
KOH	Mo	95.2	0.701	0.99	3.28
KOH	U	94.1	0.617	1.12	3.73
KOH	Se	92.4	0.544	1.27	4.23
NH_3	As	95.0	0.761	0.91	3.03
NH_3	V	93.0	0.638	1.09	3.61
NH_3	Mo	92.3	0.552	1.26	4.17
NH_3	U	90.5	0.499	1.39	4.61
NH_3	Se	88.9	0.444	1.56	5.19
$Ca(OH)_2$	As	99.0	1.187	0.58	1.94
$Ca(OH)_2$	V	98.0	1.007	0.69	2.29
$Ca(OH)_2$	Mo	96.9	0.877	0.79	2.63
$Ca(OH)_2$	U	96.1	0.781	0.89	2.95
$Ca(OH)_2$	Se	94.0	0.685	1.01	3.36

Two practical thresholds follow directly from Table 4. The D_{90} values — the dose at which the curve has covered 90 % of its range — lie between 1.9 and 5.2 g L^{-1}; by $2 \cdot D_{90}$ (4–10 g L^{-1}) the remaining headroom is below 1 %, which is why the experimental curves are flat between 6 and 10 g L^{-1} (Table 3: Mo 94→95 %, As 98→98 %). The same conclusion is reached from the

specific uptake (Table 5, Fig. 2): q for Mo in KOH-pre-treated groundwater declines from 65 μg g^{-1} at 0.5 g L^{-1} to 18 μg g^{-1} at 6 g L^{-1} and 11 μg g^{-1} at 10 g L^{-1}, so that the last 4 g L^{-1} of sorbent capture less than 1 μg of Mo per gram. Working loadings of tens of μg g^{-1} are, as expected at μg L^{-1} concentrations in a 0.1–0.2 M background, far below the mg g^{-1} capacities quoted for magnetite in concentrated solutions.

Table 5. Specific uptake q (μg g^{-1}) of Mo and U from groundwater.

Reagent	Element	0.5	1.0	2.0	4.0	6.0	8.0	10.0
KOH	Mo	65.2	55.9	41.9	25.9	18.2	13.8	11.1
NH_3	Mo	55.2	48.9	38.9	25.7	18.6	14.3	11.5
$Ca(OH)_2$	Mo	80.2	67.3	47.2	27.7	18.9	14.3	11.4
KOH	U	28.6	24.6	19.2	12.3	8.8	6.7	5.4
NH_3	U	25.9	23.3	18.4	12.6	9.3	7.2	5.8
$Ca(OH)_2$	U	36.7	30.8	22.5	13.6	9.4	7.1	5.7

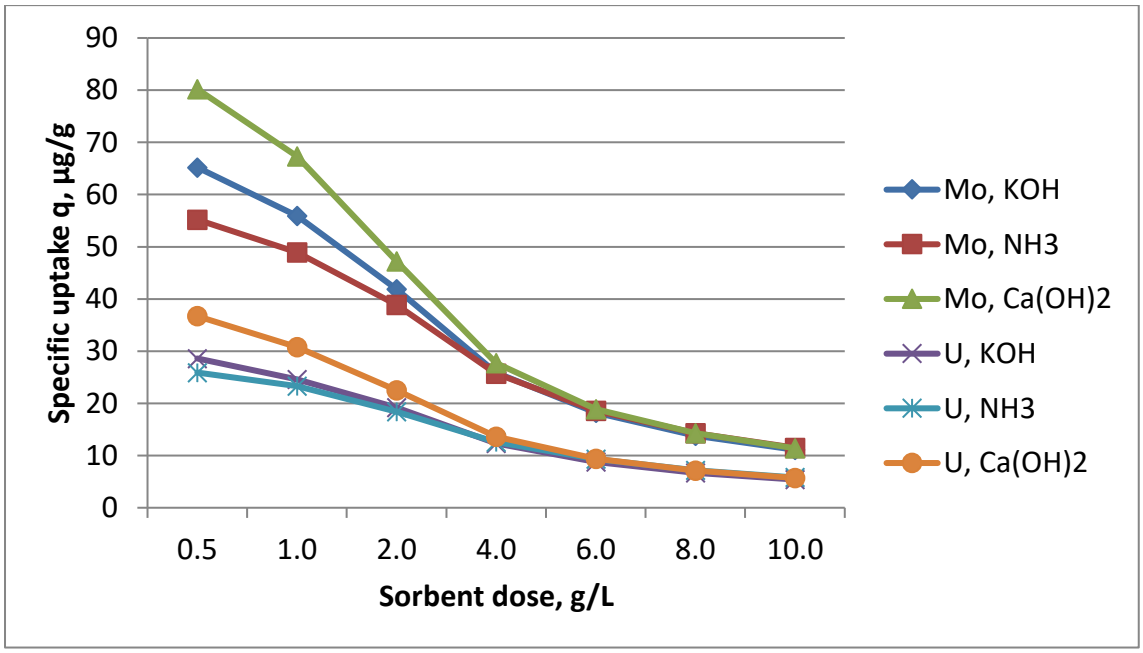


Figure 2. Specific uptake of Mo and U from groundwater versus sorbent dose for the three pre-treatment reagents.

Within each reagent series, k and η_{max} rank the elements identically: As > V > Mo > U > Se (Table 4, Fig. 3). After KOH the rate constants are 0.94, 0.81, 0.70, 0.62 and 0.54 L g^{-1}, i.e. selenium needs 1.7 times the dose that arsenic needs to reach the same fraction of its ceiling, and its ceiling is 6 points lower. The order does not change with reagent, with water or with dose — the model parameters, which integrate the whole curve, confirm what single-dose comparisons suggest.

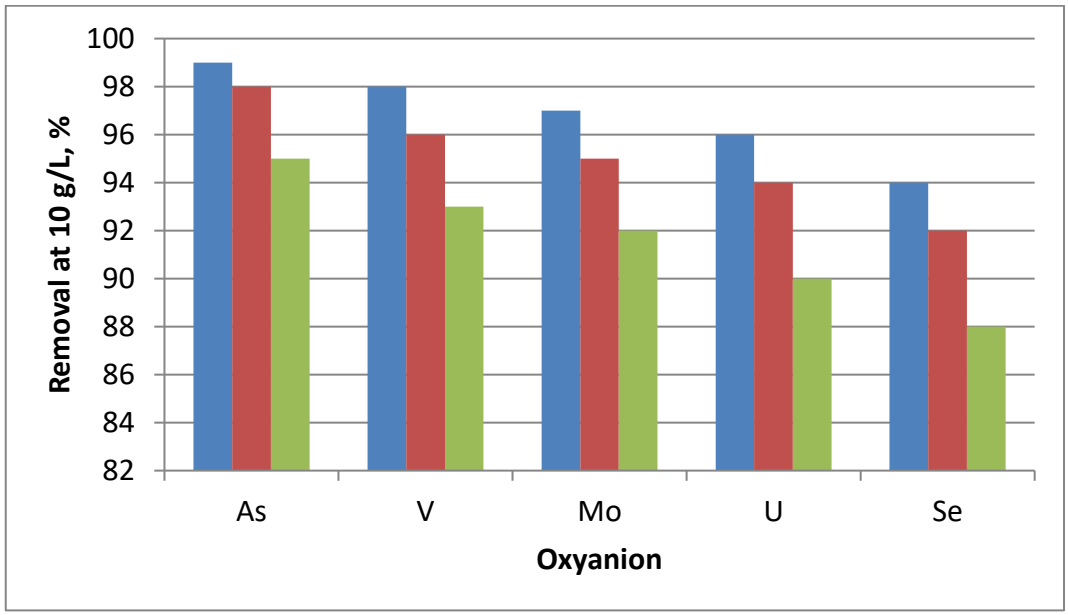


Figure 3. Removal at 10 g L^{-1} for the five oxyanions after each pre-treatment reagent.

The ranking matches the surface chemistry of the five anions on iron oxides. Arsenate and vanadate form bidentate inner-sphere complexes that are strong and nearly pH-independent between pH 4 and 8, which places them at the head of the series with D_{50} below 1 g L^{-1}. Molybdate also binds inner-sphere, but its adsorption edge falls above pH 6–7 as MoO_4^{2-} dominates and the surface loses positive charge , so at pH 7.5–8.0 it is a weaker sorbate than arsenate. Uranium is restrained not by the surface but by the solution: with 153–458 mg L^{-1} HCO_3^- and ≈550 mg L^{-1} Ca^{2+}, Ca–UO_2–CO_3 ternary complexes hold most of the U(VI) away from the surface; reduction by lattice Fe^{2+} partly offsets this and keeps uranium ahead of selenium. Selenium comes last because at the oxidising, slightly alkaline conditions of the feed a large fraction is selenate, whose outer-sphere binding is easily displaced by sulphate [20] — and sulphate is present at ≈3.6 g L^{-1}. The sorbent is thus least effective towards the anion that most resembles the dominant background anion, which is an intrinsic limitation of any iron-oxide sorbent in sulphate-rich water rather than a deficiency of this material.

The reagent used to set the pH in the first stage changes both parameters of the second stage in a consistent direction: $Ca(OH)_2$ > KOH > NH_3 for every element (Table 4). For molybdenum, k is 0.88, 0.70 and 0.55 L g^{-1} and D_{90} is 2.6, 3.3 and 4.2 g L^{-1} for the three reagents; the lime series thus reaches 90 % of its ceiling with 37 % less sorbent than the ammonia series. Because the effect acts on k, it is most visible where the curve is steep and fades where it is flat: at 2 g L^{-1} Mo removal is 80, 72 and 62 % (Fig. 4a) and U removal 76, 67 and 57 % (Fig. 4b), a spread of 18–19 points, whereas at 10 g L^{-1} the spread is 2–5 points. The reagent therefore matters in a sorbent-limited process and becomes secondary once sorbent is in excess.

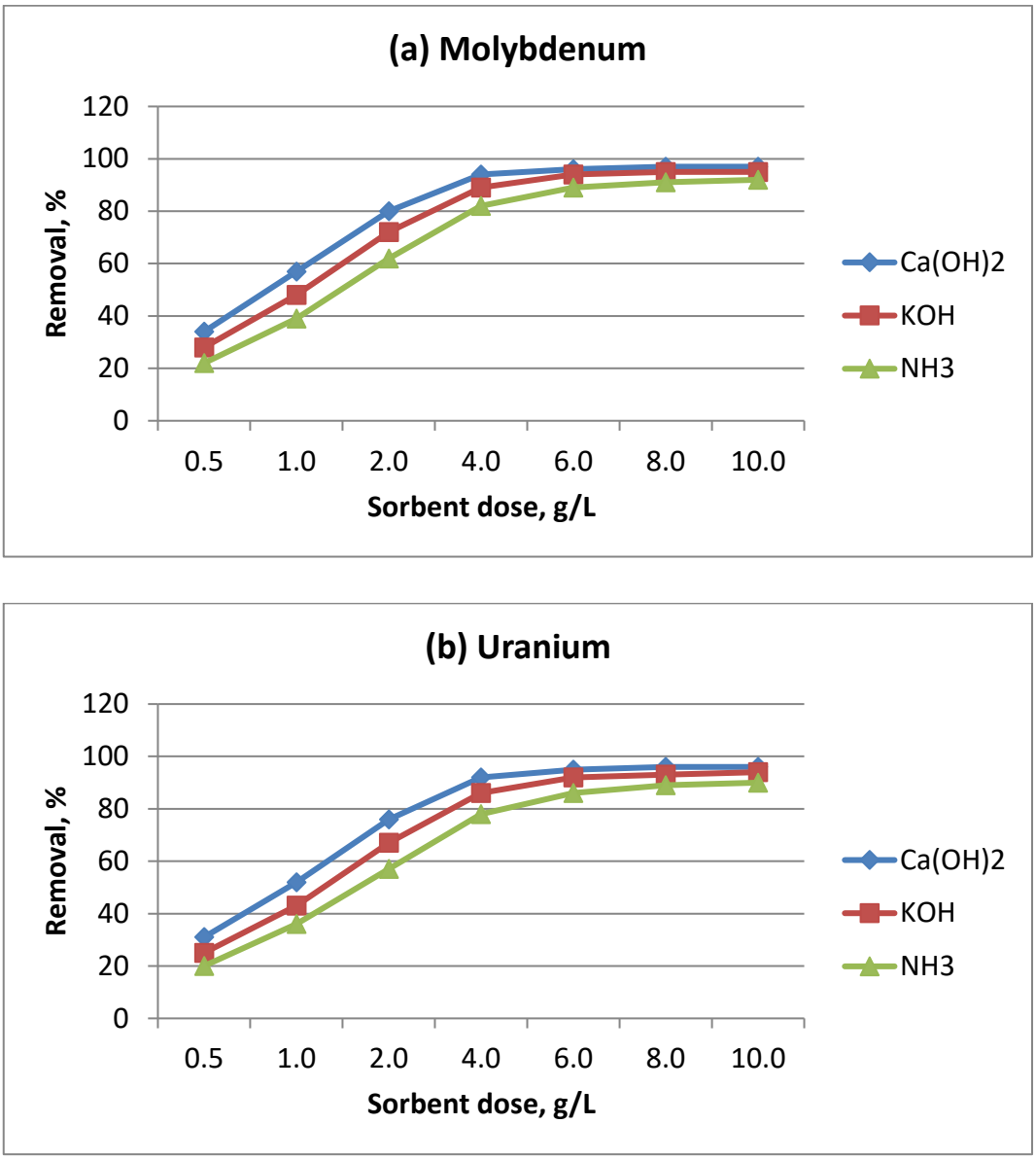


Figure 4. Removal of (a) molybdenum and (b) uranium from groundwater after KOH, NH_3 and $Ca(OH)_2$ pre-treatment.

Three mechanisms can account for the lime advantage. Lime is the only reagent that introduces Ca^{2+}; adsorbed divalent cations raise the surface charge of iron oxides and bridge anions to the surface, an effect demonstrated for arsenate on goethite in the presence of Ca^{2+} and Mg^{2+} and consistent with multi-component surface-complexation models. Lime also precipitates part of the sulphate as gypsum and part of the bicarbonate as calcite, thereby thinning out precisely the two anions that compete with selenate/molybdate and that complex uranyl. Ammonia, finally, is a weak base that must be dosed in large excess to reach pH 8, contributes no bridging cation and, judging by the slightly higher C_0 after NH_3 pre-treatment (Table 2), co-precipitates less of the oxyanions on $Fe(OH)_3$ flocs in the first stage. Since lime was also the most effective reagent for cation precipitation, it is the reagent of choice for the integrated process.

For reuse in irrigation the operative quantity is the residual concentration, which depends on the initial load as much as on η. Tables 6 and 7 give the residuals for groundwater and drainage water; Fig. 5 compares the Mo residuals in groundwater with the FAO limit.

Table 6. Residual concentrations (μg L^{-1}) in groundwater after sorption.

Reagent	Element	0.5	1.0	2.0	4.0	6.0	8.0	10.0	Limit
KOH	Mo	83.8	60.5	32.6	12.8	7.0	5.8	5.8	10
KOH	Se	19.6	15.3	9.8	4.5	2.8	2.3	2.0	20
KOH	U	42.9	32.6	18.9	8.0	4.6	4.0	3.4	30
KOH	As	4.4	2.8	1.2	0.3	0.1	0.1	0.1	10
KOH	V	2.6	1.8	0.9	0.3	0.2	0.2	0.2	—
NH_3	Mo	97.8	76.5	47.7	22.6	13.8	11.3	10.0	10
NH_3	Se	24.1	20.0	14.1	7.6	5.0	4.1	3.5	20
NH_3	U	51.7	41.4	27.8	14.2	9.1	7.1	6.5	30
NH_3	As	5.9	4.1	2.2	0.8	0.5	0.4	0.4	10
NH_3	V	3.4	2.5	1.5	0.6	0.4	0.4	0.3	—
$Ca(OH)_2$	Mo	77.9	50.7	23.6	7.1	4.7	3.5	3.5	10
$Ca(OH)_2$	Se	20.0	14.5	8.2	3.3	2.2	1.6	1.6	20
$Ca(OH)_2$	U	40.9	28.4	14.2	4.7	3.0	2.4	2.4	30
$Ca(OH)_2$	As	4.5	2.5	0.8	0.2	0.1	0.1	0.1	10
$Ca(OH)_2$	V	2.5	1.6	0.6	0.2	0.1	0.1	0.1	—

Table 7. Residual concentrations (μg L^{-1}) in drainage water after sorption.

Reagent	Element	0.5	1.0	2.0	4.0	6.0	8.0	10.0	Limit
KOH	Mo	12.3	8.9	4.8	1.9	1.0	0.9	0.9	10
KOH	Se	12.6	9.8	6.3	2.9	1.8	1.5	1.3	20
KOH	U	42.8	32.5	18.8	8.0	4.6	4.0	3.4	30
KOH	As	3.8	2.4	1.0	0.2	0.1	0.1	0.1	10
KOH	V	2.4	1.6	0.8	0.3	0.2	0.1	0.1	—
NH_3	Mo	17.0	13.3	8.3	3.9	2.4	2.0	1.7	10
NH_3	Se	16.3	13.6	9.6	5.2	3.4	2.8	2.4	20
NH_3	U	50.8	40.6	27.3	14.0	8.9	7.0	6.4	30
NH_3	As	4.9	3.4	1.8	0.7	0.4	0.4	0.4	10
NH_3	V	2.9	2.2	1.3	0.5	0.4	0.3	0.3	—
$Ca(OH)_2$	Mo	11.5	7.5	3.5	1.0	0.7	0.5	0.5	10
$Ca(OH)_2$	Se	12.1	8.8	5.0	2.0	1.3	1.0	1.0	20
$Ca(OH)_2$	U	42.3	29.4	14.7	4.9	3.1	2.5	2.5	30
$Ca(OH)_2$	As	3.5	2.0	0.6	0.1	0.1	0.1	0.1	10
$Ca(OH)_2$	V	2.2	1.4	0.5	0.1	0.1	0.1	0.1	—

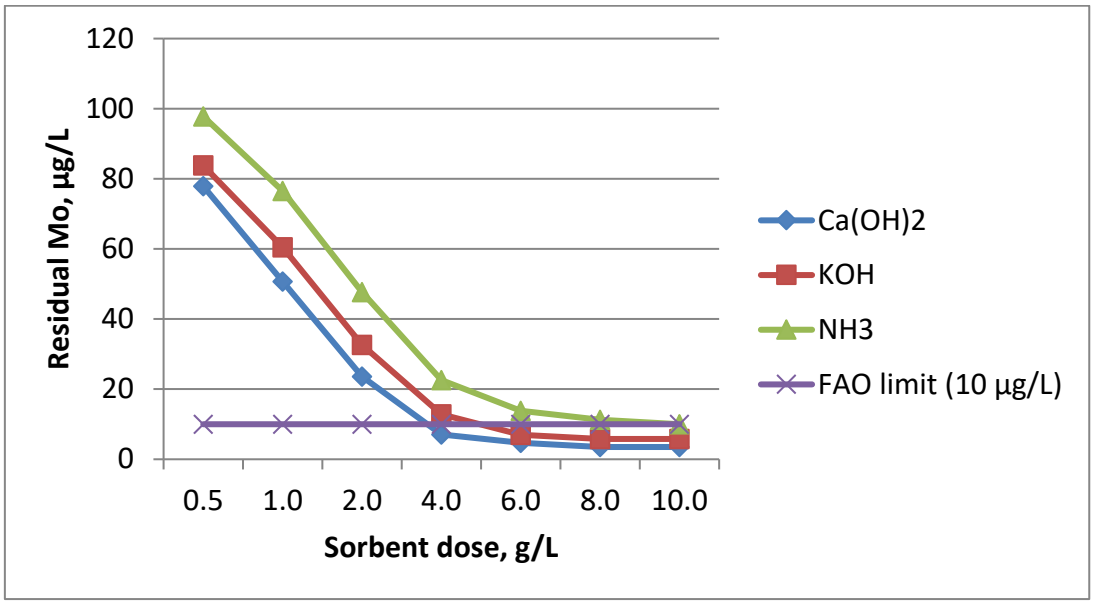


Figure 5. Residual molybdenum in groundwater versus sorbent dose for the three pre-treatment reagents, with the FAO irrigation guideline (10 µg L^{-1}).

The compliance dose can also be written in closed form. If the feed concentration is C_0 and the limit is C_L, the required removal is $\eta_L = 100(1 - C_L/C_0)$ and, from the model,

$$D_L = -\frac{1}{k}\ln\left(1 - \frac{\eta_L}{\eta_{max}}\right)$$

For molybdenum in groundwater (C_0 ≈ 116–125 µg L^{-1}, C_L = 10 µg L^{-1}, η_L ≈ 91–92 %) the equation gives D_L ≈ 3.3 g L^{-1} after lime, 4.6 g L^{-1} after KOH and 10.4 g L^{-1} after ammonia — in line with the first experimental doses that meet the limit, 4, 6 and 10 g L^{-1} (Table 8). Molybdenum is thus the limiting element for the groundwater; uranium is met at 2 g L^{-1} for all reagents, selenium at ≤1 g L^{-1} and arsenic in the feed. In the drainage water, whose Mo load is six times lower, uranium (feed 57–64 µg L^{-1}) becomes limiting and all five elements comply at 2 g L^{-1} regardless of reagent. Because removal fractions were identical for the two waters, the Mo residual curves of the drainage water lie a constant factor of ≈7 below those of the groundwater while the U curves coincide (Fig. 6).

Table 8. Lowest experimental dose (g L^{-1}) at which each element falls below its guideline.

Water	Reagent	Mo (10)	Se (20)	U (30)	As (10)	Limiting element
Groundwater	KOH	6.0	1.0	2.0	feed	Mo
Groundwater	NH_3	10.0	1.0	2.0	feed	Mo
Groundwater	$Ca(OH)_2$	4.0	0.5	2.0	feed	Mo
Drainage	KOH	1.0	feed	2.0	feed	U
Drainage	NH_3	1.0	feed	2.0	feed	U
Drainage	$Ca(OH)_2$	1.0	feed	2.0	feed	U

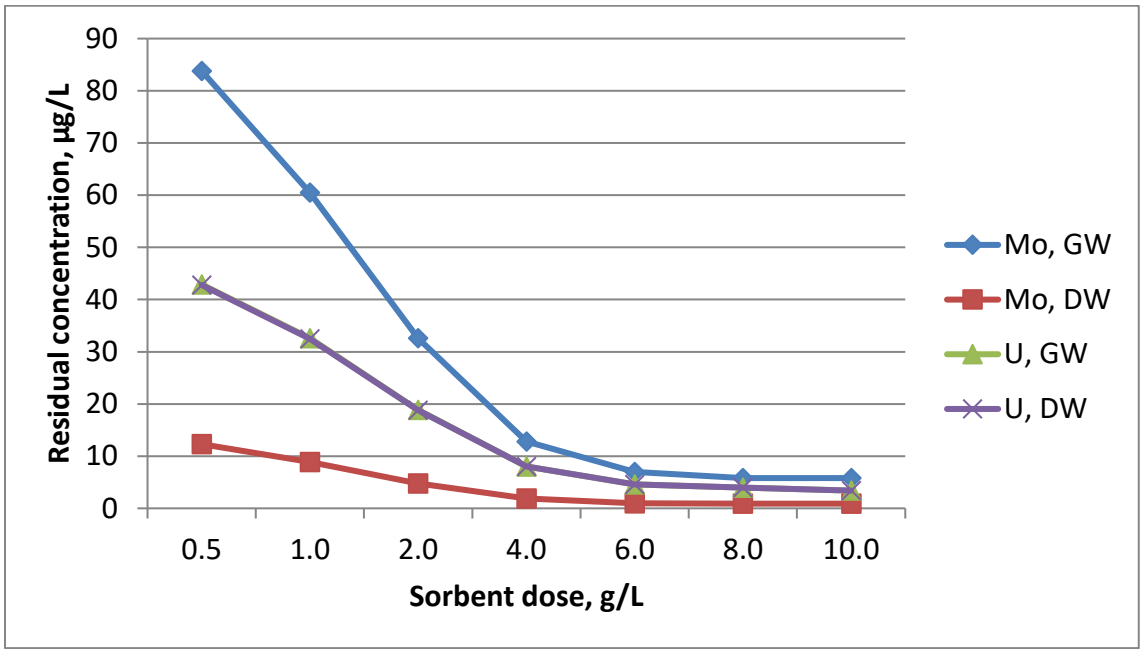


Figure 6. Residual Mo and U in groundwater (GW) and drainage water (DW) after KOH pre-treatment.

The three lines of evidence converge on a dose window of 4–6 g L^{-1} with lime pre-treatment. It lies between D_{90} and $2{\cdot}D_{90}$ for every element, so that 86–98 % removal is obtained; the specific uptake is still 18–28 µg Mo g^{-1}, i.e. the sorbent is still working rather than diluting; and the residuals of all five elements are below guideline values in both waters (for KOH pre-treatment the upper end, 6 g L^{-1}, is needed for groundwater). Going beyond 6 g L^{-1} raises sorbent consumption by up to two thirds for 1–3 points of removal; stopping at 2 g L^{-1} is sufficient for the drainage water but leaves 24–48 µg L^{-1} of Mo in the groundwater. This window, with $Ca(OH)_2$ as the first-stage reagent, is the basis of the material balance and process design of the 1000 m^3 d^{-1} scheme reported separately (sorbent make-up 0.6 kg m^{-3} with magnetic recovery and regeneration).

Two caveats apply. The treatment removes the toxic anions but not the salinity (≈8.5 g L^{-1}), so reuse must be combined with leaching, drainage, salt-tolerant crops or blending. And the data are for single-contact batch conditions; column behaviour, the effect of varying sulphate/bicarbonate ratios and the stability of k over regeneration cycles are being examined.

Discussion

The present findings demonstrate that activated Tebinbulak titanomagnetite exhibits a consistent and chemically meaningful selectivity toward the investigated oxyanions under saline water conditions. The observed affinity sequence of As > V > Mo > U > Se indicates that adsorption performance is controlled not only by sorbent dose but also by the speciation of each element and its interaction with iron-bearing surface sites. Arsenate and vanadate showed the highest removal efficiency because of their strong inner-sphere complexation with iron oxide functional groups, whereas molybdate adsorption was comparatively weaker under slightly alkaline conditions where surface protonation decreases. Uranium removal was further influenced by the presence of bicarbonate and calcium, which can stabilize soluble $Ca–UO_2–CO_3$ complexes and consequently reduce the fraction of U(VI) available for direct sorption. Selenium exhibited the lowest affinity, which can be explained by the predominance of selenate species and their relatively weak interaction with iron oxide surfaces in the presence of high sulphate concentrations. These competitive effects are particularly important because both groundwater and drainage water contained approximately 3.6 g L^{-1} sulphate, creating a chemically challenging matrix in which background anions compete for available adsorption sites.

Nevertheless, the very high goodness of fit of the saturation model ($R^2 \geq 0.999$) across the investigated dose–response curves confirms that the sorption process remained systematic and predictable despite this high ionic strength. These results therefore support the suitability of activated titanomagnetite as a robust sorbent for oxyanion removal from saline agricultural waters rather than only from simplified laboratory solutions.

The influence of the alkaline pre-treatment reagent provides further evidence that water chemistry plays a major role in determining sorption efficiency. Among the three reagents, $Ca(OH)_2$ consistently produced the highest rate constants and the lowest characteristic doses, followed by KOH and NH_3. For molybdenum, for example, the rate constant increased from 0.552 L g^{-1} with NH_3 to 0.701 L g^{-1} with KOH and 0.877 L g^{-1} with $Ca(OH)_2$, while the corresponding D_{90} decreased from 4.17 to 3.28 and 2.63 g L^{-1}, respectively. This improvement may be attributed to several simultaneous mechanisms, including Ca^{2+}-mediated surface bridging, partial precipitation of sulphate as gypsum, and removal of bicarbonate through calcite formation, all of which decrease competition for active sites. In contrast, NH_3 does not supply a divalent bridging cation and appears to remove less of the competing species during the first treatment stage. The stronger performance of $Ca(OH)_2$ is therefore not merely a pH effect but reflects a beneficial modification of both sorbent–solute interactions and the composition of the treated water. This finding is operationally important because the advantage of lime is greatest at low to intermediate sorbent doses, where sorbent efficiency and treatment cost are most sensitive to process conditions. Consequently, $Ca(OH)_2$ can be considered the most appropriate pre-treatment reagent for an integrated precipitation–adsorption system using Tebinbulak titanomagnetite.

From an application perspective, the results also show that removal percentage alone is insufficient for selecting an operating dose because compliance depends strongly on the initial concentration of each element. Molybdenum was the limiting contaminant in groundwater because its initial concentration was substantially higher than the irrigation guideline, whereas uranium became the limiting element in drainage water. In groundwater, the molybdenum guideline was achieved experimentally at 4 g L^{-1} after $Ca(OH)_2$ pre-treatment, 6 g L^{-1} after KOH, and 10 g L^{-1} after NH_3, while uranium in drainage water reached compliance at only 2 g L^{-1} regardless of reagent. These differences demonstrate that an identical percentage removal may produce very different residual concentrations when initial contaminant loads differ. At the same time, increasing the sorbent dose beyond approximately 6 g L^{-1} produced only marginal improvement because the adsorption curves approached their asymptotic removal limits and the specific uptake per gram of sorbent declined sharply. The combined evidence from characteristic dose, residual concentration, and specific uptake therefore supports an operating window of 4–6 g L^{-1} with $Ca(OH)_2$ pre-treatment as the most efficient compromise between treatment performance and sorbent utilization. This operating range is sufficient to bring all investigated oxyanions below the relevant guideline values in both waters while avoiding unnecessary sorbent consumption. However, because the process does not remove the high background salinity and the current experiments were conducted under batch conditions, further validation under continuous-flow conditions, different sulphate/bicarbonate ratios, and repeated regeneration cycles remains necessary before full-scale implementation.

Conclusion

The batch removal of Mo, Se, U, As and V from pre-treated (pH 7.5–8.0) saline groundwater and drainage water by activated Tebinbulak titanomagnetite is described, for all 42 dose–response curves, by $\eta = \eta max(1 - e{-}kD)$ with $R^2 \geq 0.999$; ηmax = 89–99 % and k = 0.44–1.19 L g^{-1}.

The rate constant ranks the oxyanions invariably as As > V > Mo > U > Se (D_{90} = 2.4–4.2 g L^{-1} after KOH), consistent with inner-sphere binding of arsenate and vanadate, the pH-limited sorption of molybdate, the sequestration of U(VI) in Ca–UO_2–CO_3 complexes and the sulphate-

sensitive, largely outer-sphere binding of selenate.

The pre-treatment reagent shifts k in the order $Ca(OH)_2$ > KOH > NH_3 (0.88, 0.70, 0.55 L g^{-1} for Mo), attributable to Ca^{2+} bridging and to removal of competing sulphate and bicarbonate by lime; the effect is largest at low dose and fades at high dose.

Molybdenum limits the groundwater (feed 116–125 µg L^{-1}): the FAO limit is met at 4 g L^{-1} after lime, 6 g L^{-1} after KOH and 10 g L^{-1} after ammonia; uranium limits the drainage water and is met at 2 g L^{-1}.

A dose of 4–6 g L^{-1} with lime pre-treatment brings all five elements below FAO/WHO guidelines in both waters while keeping specific uptake at 18–28 µg Mo g^{-1}, and is recommended as the operating window for returning these waters to irrigation.

References

[1] M. Qadir, B. R. Sharma, A. Bruggeman, R. Choukr-Allah, and F. Karajeh, "Non-conventional water resources and opportunities for water augmentation to achieve food security in water scarce countries," Agricultural Water Management, vol. 87, pp. 2–22, 2007, doi: 10.1016/j.agwat.2006.03.018.

[2] K. K. Tanji and N. C. Kielen, Agricultural Drainage Water Management in Arid and Semi-Arid Areas, FAO Irrigation and Drainage Paper 61. Rome, Italy: FAO, 2002.

[3] P. Micklin, "The Aral Sea disaster," Annual Review of Earth and Planetary Sciences, vol. 35, pp. 47–72, 2007, doi: 10.1146/annurev.earth.35.031306.140120.

[4] R. Kulmatov, J. Mirzaev, J. Abuduwaili, and B. Karimov, "Challenges for the sustainable use of water and land resources under a changing climate and increasing salinization in the Jizzakh irrigation zone of Uzbekistan," Journal of Arid Land, vol. 12, pp. 90–103, 2020, doi: 10.1007/s40333-020-0092-8.

[5] R. S. Ayers and D. W. Westcot, Water Quality for Agriculture, FAO Irrigation and Drainage Paper 29, Rev. 1. Rome, Italy: FAO, 1985.

[6] World Health Organization (WHO), Guidelines for Drinking-Water Quality, 4th ed., incorporating the 1st addendum. Geneva, Switzerland: WHO, 2017.

[7] H. M. Ohlendorf, D. J. Hoffman, M. K. Saiki, and T. W. Aldrich, "Embryonic mortality and abnormalities of aquatic birds: Apparent impacts of selenium from irrigation drainwater," Science of the Total Environment, vol. 52, pp. 49–63, 1986, doi: 10.1016/0048-9697(86)90104-X.

[8] T. S. Presser and H. M. Ohlendorf, "Biogeochemical cycling of selenium in the San Joaquin Valley, California, USA," Environmental Management, vol. 11, pp. 805–821, 1987, doi: 10.1007/BF01867247.

[9] R. Tornqvist, J. Jarsjo, and B. Karimov, "Health risks from large-scale water pollution: Trends in Central Asia," Environment International, vol. 37, pp. 435–442, 2011, doi: 10.1016/j.envint.2010.11.006.

[10] A. Baubekova, A. Akindykova, A. Mamirova, C. Dumat, and S. Jurjanz, "Evaluation of environmental contamination by toxic trace elements in Kazakhstan based on reviews of available scientific data," Environmental Science and Pollution Research, vol. 28, pp. 43315–43328, 2021, doi: 10.1007/s11356-021-14979-z.

[11] J.-H. Huang, F. Huang, L. Evans, and S. Glasauer, "Vanadium: Global (bio)geochemistry," Chemical Geology, vol. 417, pp. 68–89, 2015, doi: 10.1016/j.chemgeo.2015.09.019.

[12] J. P. Gustafsson, "Vanadium geochemistry in the biogeosphere—Speciation, solid-solution interactions, and ecotoxicity," Applied Geochemistry, vol. 102, pp. 1–25, 2019, doi: 10.1016/j.apgeochem.2018.12.027.

[13] D. Mohan and C. U. Pittman, "Arsenic removal from water/wastewater using adsorbents—A critical review," Journal of Hazardous Materials, vol. 142, pp. 1–53, 2007, doi: 10.1016/j.jhazmat.2007.01.006.

[14] C.-K. D. Hsi and D. Langmuir, "Adsorption of uranyl onto ferric oxyhydroxides: Application of the surface complexation site-binding model," Geochimica et Cosmochimica Acta, vol. 49, pp. 1931–1941, 1985, doi: 10.1016/0016-7037(85)90088-2.
[15] C. A. Hejase, K. A. Weitzel, S. C. Stokes, et al., "Opportunities for treatment and reuse of agricultural drainage in the United States," ACS ES&T Engineering, vol. 2, pp. 292–305, 2022, doi: 10.1021/acsestengg.1c00277.
[16] W. Dong and S. C. Brooks, "Determination of the formation constants of ternary complexes of uranyl and carbonate with alkaline earth metals (Mg^{2+}, Ca^{2+}, Sr^{2+}, and Ba^{2+}) using anion exchange method," Environmental Science & Technology, vol. 40, pp. 4689–4695, 2006, doi: 10.1021/es0606327.
[17] B. D. Stewart, M. A. Mayes, and S. Fendorf, "Impact of uranyl–calcium–carbonato complexes on uranium(VI) adsorption to synthetic and natural sediments," Environmental Science & Technology, vol. 44, pp. 928–934, 2010, doi: 10.1021/es902194x.
[18] B. A. Manning, S. E. Fendorf, and S. Goldberg, "Surface structures and stability of arsenic(III) on goethite: Spectroscopic evidence for inner-sphere complexes," Environmental Science & Technology, vol. 32, pp. 2383–2388, 1998, doi: 10.1021/es9802201.
[19] S. Goldberg and C. T. Johnston, "Mechanisms of arsenic adsorption on amorphous oxides evaluated using macroscopic measurements, vibrational spectroscopy, and surface complexation modeling," Journal of Colloid and Interface Science, vol. 234, pp. 204–216, 2001, doi: 10.1006/jcis.2000.7295.
[20] D. Peak and D. L. Sparks, "Mechanisms of selenate adsorption on iron oxides and hydroxides," Environmental Science & Technology, vol. 36, pp. 1460–1466, 2002, doi: 10.1021/es0156643.